Journal of Constructional Steel Research 137 (2017) 180–191

Contents lists available at ScienceDirect

Journal of Constructional Steel Research

journal homepage: www.elsevier.com/locate/jcsr

Experimental investigation of panel zone in rigid beam to box column connection

Ebrahim Jahanbakhti[a], Nader Fanaie[a,*], Alireza Rezaeian[b]

[a] Department of Civil Engineering, K.N. Toosi University of Technology, Tehran, Iran
[b] Department of Civil Engineering, Karaj Branch Islamic Azad University, Karaj, Iran

ARTICLE INFO

Keywords:
Experimental investigation
Rigid connection
Continuity plate
Yield lines theory
Box column

ABSTRACT

This research presents the results of an experimental effort conducted on three full-scale rigid connections between I-beam and box-column. Accordingly, it is focused on the elimination of continuity plates from such connections through controlling the thickness of column flange. The appropriate thickness is determined by analytical method and then verified through experimental investigations of three different full-scale connections under AISC protocol of cyclic loading. Pre-qualified connections, presented in AISC (WUF-W) are selected for the test. They have the beam flange width to column flange width ratios of 0.53, 0.6 and 0.8, and beam flange width to beam depth ratios of 0.48, 0.72 and 0.65. According to the obtained results, panel zone remains elastic in all tested samples; and plastic hinges are formed in the beam and near the column flange. Moreover, the samples reach to the 6% story drift before experiencing the permissible strength degradation. Therefore the tested connections have satisfied criteria of special moment resisting frame (SMRF) according to AISC. According to the FEMA requirements for SMRF, no crack should be observed in the connection up to the story drift of 4%. However, in a sample of this experimental research, crack is observed in story drift of 3%.

1. Introduction

Column stiffener connections were used with full penetration groove weld and conservative design in the moment steel frames before Northridge earthquake (1994). The intention to conservatively design of such connections, regarding their significant effects on the distribution of strain and stress in the panel zone, resulted in their installations where no continuity plates were needed, even with the thickness over than needed. These plates are connected to the column flange by full penetration groove weld. Such welds are apt to the stress concentration and usually experience cracks in the root during execution. The flexural connections between beams and columns mostly experienced weld fractures in the Northridge earthquake [1]. In 1997–2002, the seismic guidelines pointed out the necessity of installing stiffeners and removing the design criteria [2]. Accordingly, more concise discussions are found about the stiffeners in the version 1999 of AICS seismic code, comparing to its previous versions, and more detailed in the following one [3]. Tremblay et al. studied the connection failure in the Northridge earthquake, comparing it with the expected behavior, and recommended using the continuity plates in the flexural connections [4]. Kaufmann et al. focused on the brittle or ductile behavior of connections and expressed that the connections with electrodes of higher stiffness and continuity plates have more frangible behaviors [5]. Reoder applied finite element analysis and verified the improvement of stress distribution in the connection region with installing continuity plates [6]. Yee et al. recommended fillet weld instead of full penetration groove weld for preventing brittle fractures [7]. Engelhardt studied several beam to column connections with reduced beam sections and recommended the same thickness of beam flange for continuity plate [8]. Ricles expressed that the connection showed better seismic behavior in case of continuity plate installation; however, this installation could be ignored if the column flange had sufficient thickness [9]. Ghobadi et al. studied experimentally and analytically two single-sided full scale I-beam to box-column connections with the development of detail of T-stiffeners added to existing moment connections and resulted specimens with new proposed procedure performed well during test and also no crack propagation was seen [10]. Kiamanesh et al. investigated both experimentally and analytically the effect of stiffeners (column stiffeners, side-stiffeners, top and bottom flange stiffeners) and also effect of column flange thickness on the connection performance and energy dissipation. The specimens with both column and top-flange stiffeners had the highest values of energy dissipation. Decreasing the column thickness, in general, results in the decrease of connection stiffness and the increase of stress. Moreover, higher values of plastic

* Corresponding author at: K.N. Toosi University of Technology, Civil Engineering Department, No. 1346, Vali-Asr Street, P.O. Box. 15875-4416, 19697 Tehran, Iran.
E-mail address: fanaie@kntu.ac.ir (N. Fanaie).

http://dx.doi.org/10.1016/j.jcsr.2017.06.025
Received 6 May 2016; Received in revised form 19 April 2017; Accepted 24 June 2017

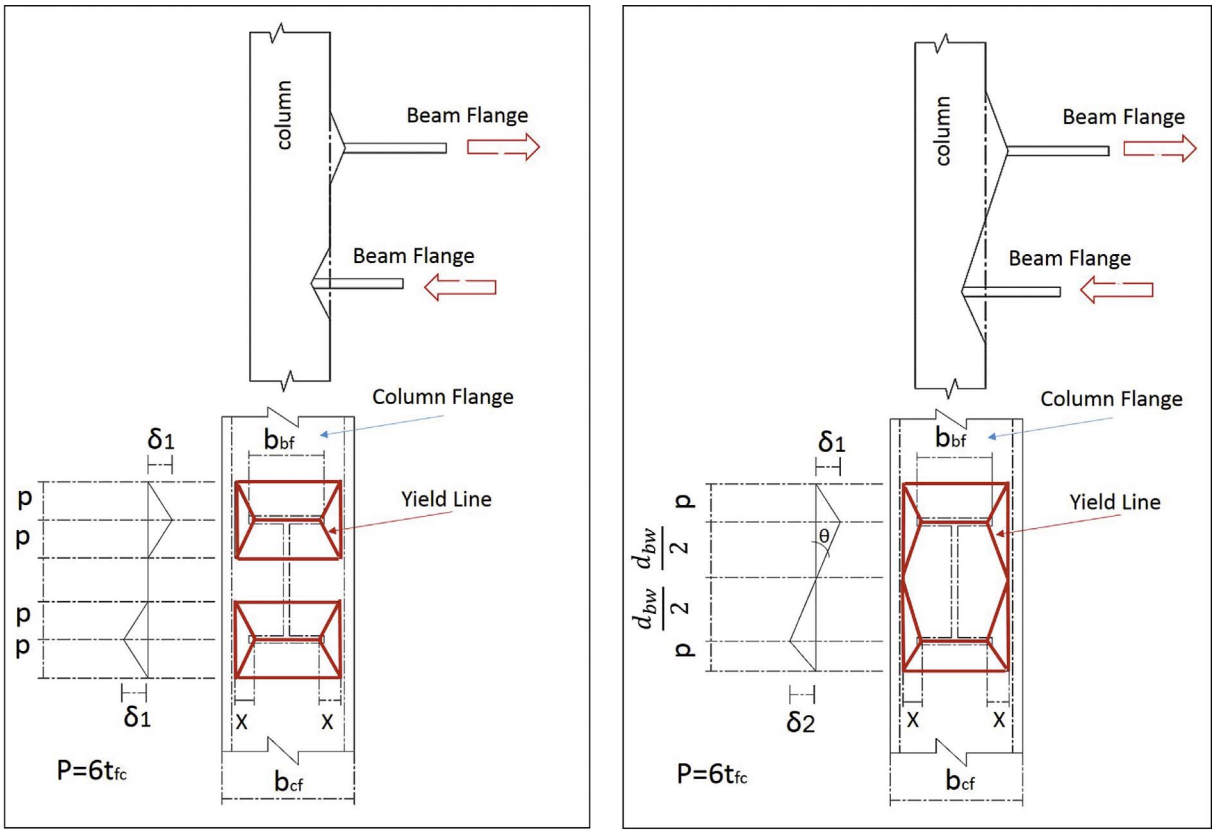

Fig. 1. Yielding mechanism: a) first mechanism; b) second mechanism.

Table 1
The specifications of the samples tested by Saneei Nia et al. [16].

Specimen	b_f (cm)	t_f (cm)	d_b (cm)	t_w (cm)	d_c (cm)	t_c (cm)	$\Sigma M_{pc}/\Sigma M_{pb}$
DC-S	16	1.5	33	0.8	30	1.5	1.03
DC-M	24	1.5	33	0.8	40	2.0	1.34
DC-L	24	2.0	38	0.8	50	2.5	1.74

Table 2
The thickness needed for column flange in case of not installing the continuity plates.

Column flange thickness	Sp-S	Sp-M	Sp-L
Needed thickness with respect to the first mechanism (mm)	30	36.7	42.3
Needed thickness with respect to the second mechanism (mm)	26.5	33.7	37.9
The used thickness (mm)	30	35	45

strain are observed in the side-stiffeners in case of removing column stiffener [11]. Mirghaderi et al. proposed a new moment connection for connecting I-beam to Box-column consisting of a vertical through plate instead of continuity plates. They studied two cyclically loaded specimens and suggested a design method to determine the dimension of through plate and also to evaluate the seismic performance of proposed connection. The specimens reached at least 0.06 rad of total story drift before experiencing strength degradation during the test [12]. Torabian et al. proposed an I-beam to Box-column moment connection without continuity plates consisting of vertical plates passed through the diagonal axes of a square box-column and welded to the box corners. Two cyclically loaded specimens were tested to evaluate the seismic performance of the connection. The obtained results showed that the specimens reached the 0.06 rad total story drift; and the proposed connection could be used as a prequalified connection in the special moment resisting frames [13]. The requirements of continuity plate installation in the panel zone were primarily presented by Graham et al. The studies with the purpose of stiffener requirements and rotation capacity were conducted on the two-way and four-way interior I-beam to I-column connections with typical sizes in the building frames. The results obtained for monotonically loaded specimens showed that stiffeners might be omitted in many beam to column connections. A formula was derived to control the stiffening requirements in I-beam to I-column connections by use of theoretical analysis, tests results and typical connections in building frames [14].

2. Analytical calculation of loading capacity of box column flange

Several clauses are presented in AISC-341-10 for controlling the requirements of installing continuity plates in the connections of I-shape beam to I-shape and boxed I-shape columns [15]. These relations are respectively results of analytical and laboratory investigations of Graham et al. and those of laboratory investigations of Ricles et al. [9,14]. Graham applied yield lines theory for the flange of I-shape column to calculate loading capacity. He considered several assumptions and calculations in his analysis with respect to the applicable connections. Following the attempts and calculations of Graham, in this research, two possible mechanisms, presented in Fig. 1a & b, are investigated based on the yield lines theory.

2.1. Analytical calculation through the first mechanism

Based on yield line theory the local bending resistance capacity of column flange (Q) for the first mechanism shown in Fig. 1a is calculable by equating the external work due to beam flange force on column flange calculated in Eq. (1) with internal work due to the yield lines

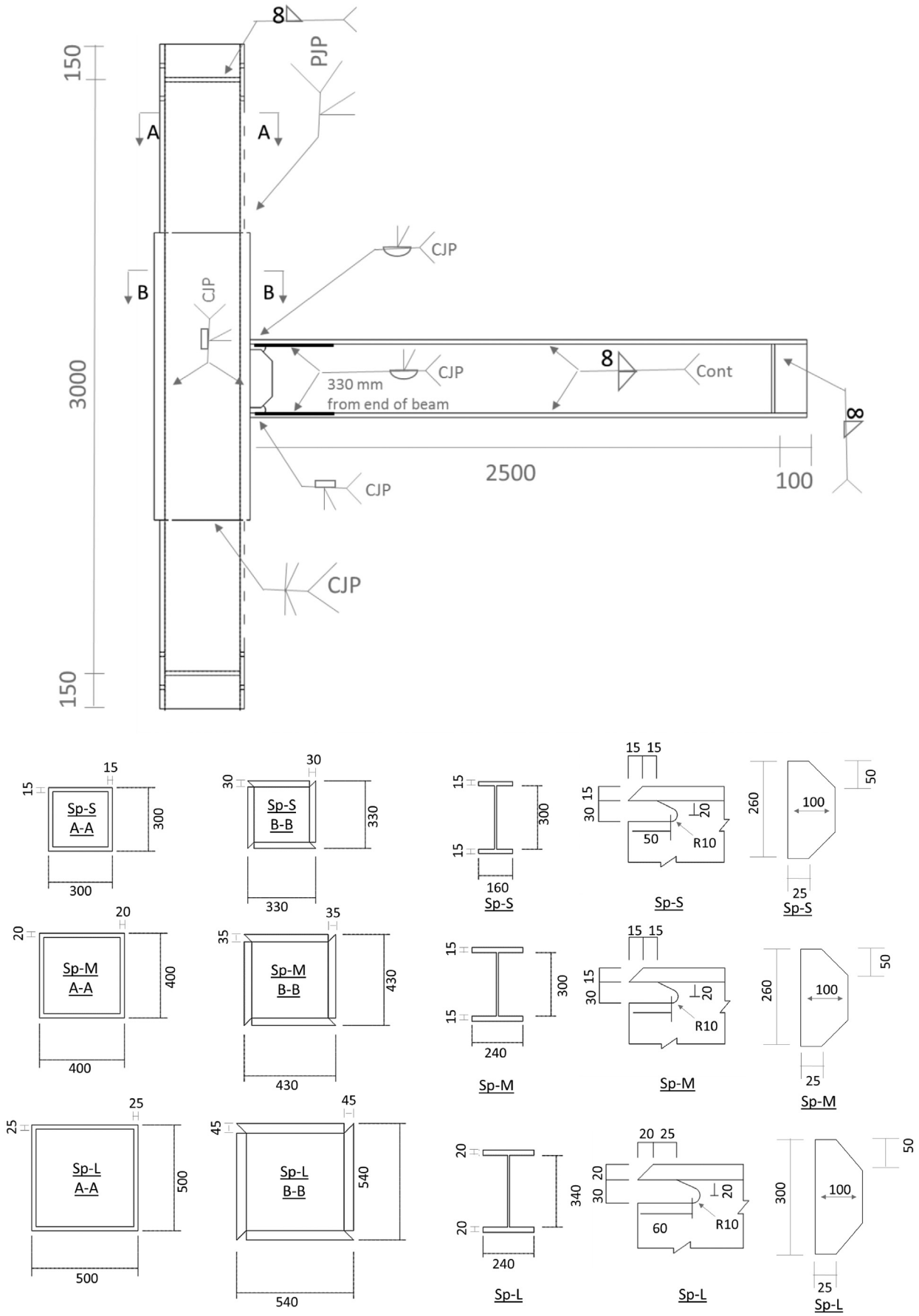

Fig. 2. The execution map of tested samples (unit: mm).

Fig. 3. Assembling the column in the factory: a) assembling the column's U; b) covering the U with fourth plate; c) assembling the beam to the column.

Table 3
Mechanical specifications of the plates used in the construction.

Thickness (mm)	F_y (MPa)	F_u (MPa)	Elongation (%)
8	289.5	382.3	27.7
10	279.3	355.5	27.1
15	250	379.1	28.2
20	268	381.9	26.5
25	272.5	442.1	25.8
30	259	412.4	27.2
35	282	461.3	26.4
45	280	390.4	26

forming in the column flange calculated in Eq. (2) as we know the plastic moment of a plate (M_p) with thickness of t_p and yield strength of F_y is equal to $\frac{1}{4}t^2F_y$ and finally by some math calculation the local bending resistance capacity of column flange calculated as Eq. (3).

$$W_{ext} = \left(\frac{Q}{b_{bf}}\right)\left[(b_{cf} - 2x) + 2\left(0.5*\frac{(b_{bf} - (b_{cf} - 2x))}{2}\left(1 + \frac{b_{cf} - b_{bf}}{2x}\right)\right)\right] \tag{1}$$

$$W_{int} = 4M_p\left[\frac{2b_{cf}}{6t_{cf}} + \frac{6t_{cf}}{x}\right] \tag{2}$$

$$Q = Ct_{cf}^2F_{yc} \tag{3}$$

Where, C factor includes the geometrical specifications of connection, t_{cf} is the column flange thickness and F_{yc} is the column flange yield strength. Values of 6.25 to 7 are obtained for C factor in applicable connections and 6.25 is considered for conservative status. The studied applicable connections have different ratios of beam flange width to column flange width (0.5 to 0.9) and different ratios of column flange thickness to beam flange width (0.05 to 0.2). The capacity loading, transmittable from beam flange, as Graham used engineering judgment to conservatively reduce the resistance of column flange by 20% is considered 80% of local bending resistance capacity of column flange, calculated by yield lines theory, and expressed as follows:

$$R_n = 0.8(Ct_{cf}^2F_{yc}) \tag{4}$$

In the seismic design, $R_n = 1.8F_yt_{bf}b_{bf}$ is considered as the siesmic load transmittable from beam flange to column where t_{bf} is beam flange thickness and b_{bf} is beam flange width. The factor of 1.8 in seismic load is obtained from multiplying the strain hardening factor of 1.3 by 1.4 due to the assuming of beam flanges as load transmitter components. Accordingly, Eq. (3) is obtained for controlling the local bending of box column flange in the connection with I-shape beam.

$$t_{cf} \cong 0.4\sqrt{1.3\left(1.8t_{bf}b_{bf}\frac{F_{yb}}{F_{yc}}\right)} = 0.46\sqrt{1.8t_{bf}b_{bf}\frac{F_{yb}}{F_{yc}}} \tag{5}$$

2.2. Analytical calculation through the second mechanism

Concerning the second mechanism, presented in Fig. 1b, yield lines theory is used to solve the problem. The external work caused by beam flange force is applied to the column flange and calculated by Eq. (6). The internal work due to the yield lines is formed in the column flange and calculated by Eq. (7). Like previous mechanism, local bending resistance capacity of column flange is calculated by Eq. (4) through equating the external work with the internal one. In this mechanism, the loading capacity transmittable from beam to column is considered 80% of local bending resistance capacity of column flange like the previous mechanism. However, unlike the first mechanism, the effect of beam web is considered in load transmission in the second one. Besides, only the factor of 1.3 is used for calculating the seismic load due to strain hardening. It means that $R_n = 1.3F_yt_{bf}b_{bf}$ is considered as the value transmittable from beam to column flange, regarding the transmittable load from the flange and web of the beam. Therefore, Eq. (6) is obtained for controlling the local bending of box column flange in the connection with I-shape beam where t_{bw} is beam web thickness, d_{bw} is beam web depth, d_b is beam depth and b_{fc} is column flange width.

$$W_{int} = 2M_p\left[\frac{2b_{cf}}{6t_{cf}} + \frac{b_{cf}}{d_{bw}/2} + \frac{4(6t_{cf} + d_{bw}/2)}{x}\right] \tag{6}$$

$$W_{ext} = 2\left(\frac{Q}{b_{bf} + d_{bw}/2}\right)\left[(b_{cf} - 2x) + \frac{d_{bw}/2}{2} + 2\left(0.5*\frac{(b_{bf} - (b_{cf} - 2x))}{2}\left(1 + \frac{b_{cf} - b_{bf}}{2x}\right)\right)\right] \tag{7}$$

$$Q = Ct_{cf}^2F_{yc} \tag{8}$$

$$R_n = 0.8(Ct_{cf}^2F_{yc}) \tag{9}$$

$$t_{cf} \cong 0.4\sqrt{10.14\frac{\left(F_{yf}t_{bf}b_{bf} + F_{yw}t_{bw}\frac{d_{bw}}{2}\right)}{F_{yc}\left[3\frac{d_b}{b_{fb}} + 6\frac{b_{fb}}{b_{fc}} - 0.5\right]}} \tag{10}$$

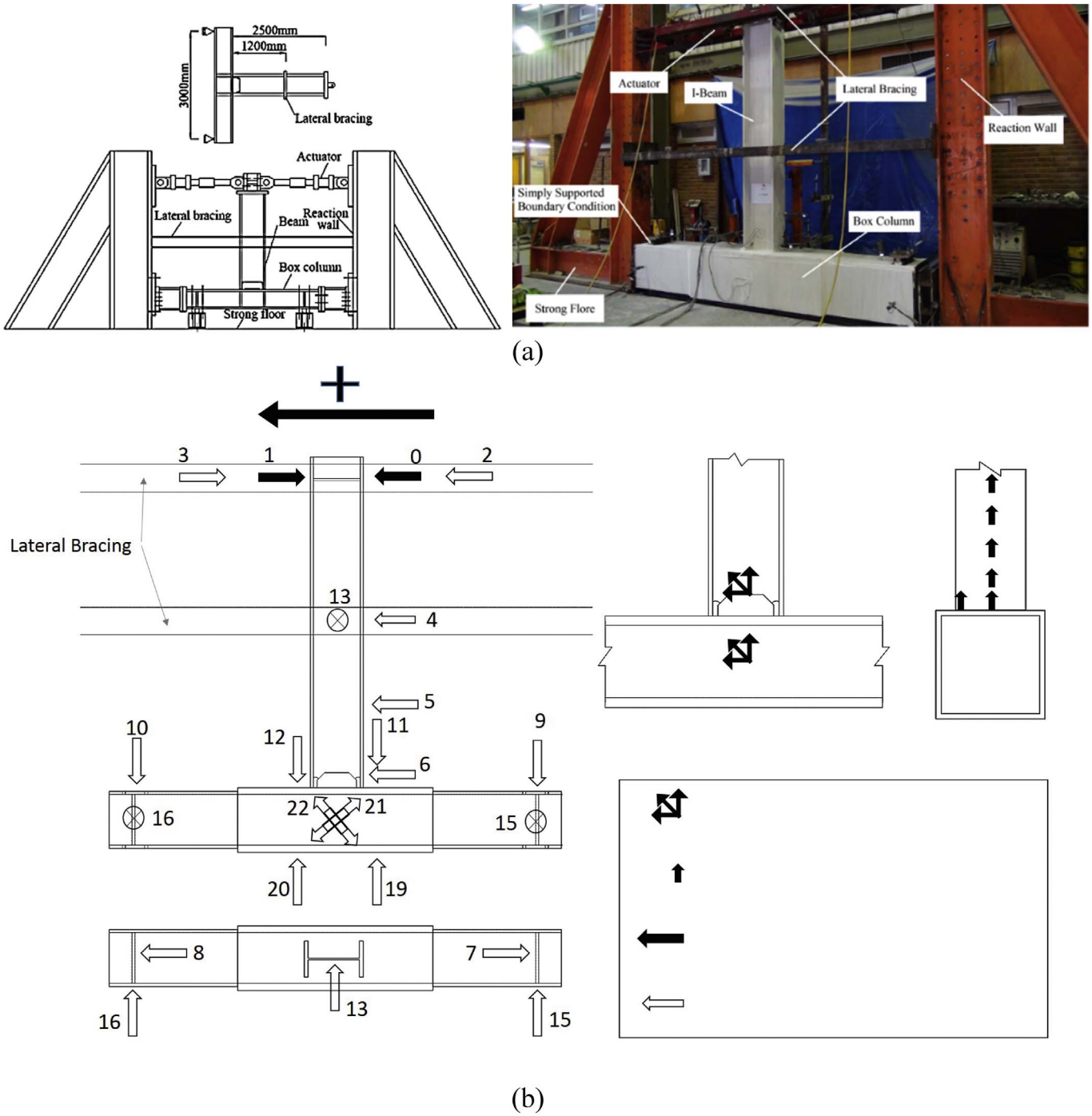

Fig. 4. a) Configuration of the test; b) instrumentation in the laboratory.

3. Laboratory investigations

3.1. Test specimens selection

The samples considered for laboratory tests are those tested by Saneei Nia et al. [16]. They tested some specimens to investigate the seismic performance of WUF-W connection. These samples are direct rigid connections of I-shape beams with constant sections to the box columns with continuity plates in three sizes of small, medium and large. They are selected from side nodes of the second story of 7-, 12- and 20-story buildings with the geometrical size shown in Table 1. The columns are simply supported in both sides and two hydraulic jacks are placed at the beam end to apply AISC cyclic loading protocol. According to experimental results presented by Saneei Nia, special moment frame criteria are satisfied by this type connection of beam to box column. Therefore, their tested specimens are chosen for this research.

3.2. Redesigning of selected specimens

Considering Table 2, the thickness of column flange plates in the selected connections satisfies none of the equations Eqs. (5) & (10) which are derived analytically. Therefore, in this research, the used plates for constructing the samples are chosen among manufacturing thickness with engineering judgment to control the derived equations. Based on the map, presented in Fig. 2, the plates are used with the

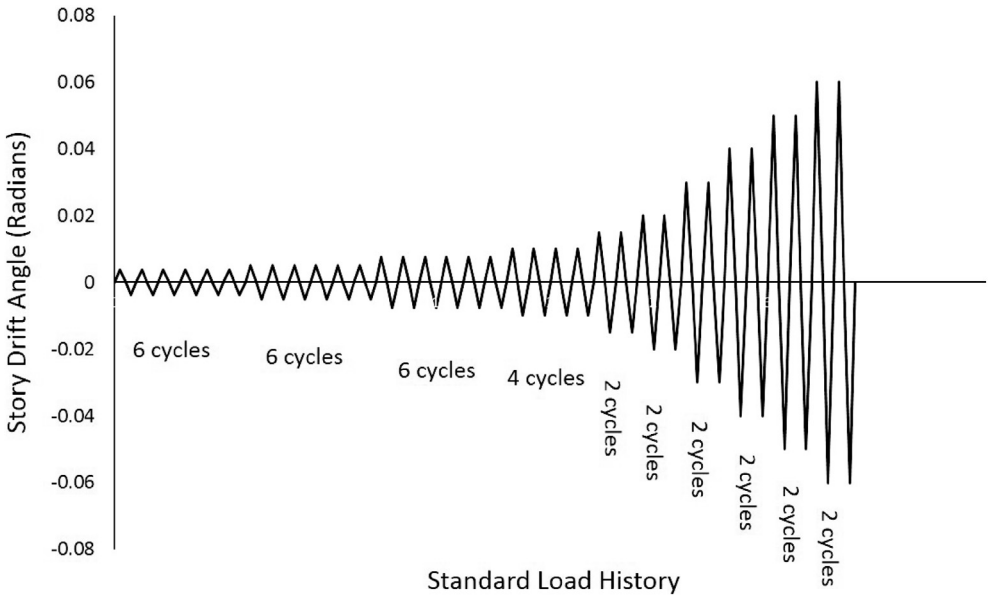

Fig. 5. The history of AISC-341-10 loading.

thickness of 30 mm, 35 mm and 45 mm for Sp-S, Sp-M and Sp-L samples, respectively. Also the shape and geometry size of weld access holes are turned to seismic recommends. Fig. 3 shows the assembling of the column without continuity plate as well as beam to column connection. The plates with equal thickness, used in the construction of samples, are prepared from one sheet. The sample for each thickness has also provided by the same sheet and subjected to tensile testing. Table 3 presents the results obtained from tensile tests of the plates.

3.3. Configuration of the test

The objective of this research is to investigate the seismic performance of I-beam to box column rigid connection without continuity plates. Accordingly, the specimens are selected from Saneei Nia's studies; and then test configuration and instrumentation of 3 laboratory samples are setup according to Fig. 4. The purpose is to meet appropriate behavior of the connection subjected to cyclic loading and assess the creation and progression of the crack practically. Both ends of the column are closed by hinged supports. The beam is laterally braced at the distance of 1200 mm from column face. The beam end, where the hydraulic jacks are placed, is laterally braced as well. The load cells are located in the direction of hydraulic jacks to measure the horizontal load applied to the beam end. Two LVDTs are placed to control the displacement of beam end; and their average measures is considered as beam end displacement to increase the accuracy. In both ends of column, three LVDTs are located for each hinge support to control the unintended displacement at the column ends. Shear distortion of panel zone is measured by two diagonal LVDTs, and strain distribution by pasting two types of strain gauges on the beam flange, web and panel zone. A whitewash is painted on the specimens to monitor inelastic deformation of connection components during the test.

4. Loading history

Fig. 5 presents the applied cyclic loading protocol according to AISC-341-10. This cyclic load is applied to the end of beam by controlling the hydraulic jack displacement followed the loading history which consists the gradual increase of cycles.

4.1. Laboratory observations

The laboratory observations of 3 tested samples are briefly presented in the following one by one:

4.1.1. Sp-S sample

The first sign of whitewash flaking is observed on the beam flange in the story drift of 0.75%, Fig. 6. By continuing the test, this flaking approaches from sides to the middle of flange and increases near connection region. The first whitewash flaking on the beam web is observed in the 3% drift and above the shear plate of web. During sample loading in the 4% drift, crack is observed in the region between base metal and weld in the connection region of beam flange to column, Fig. 7. In the first cycle of 5% drift, slight buckling is observed in the compressive flange of beam. The crack is opened in the back loading of the same cycle and the test is finished.

4.1.2. Sp-M sample

In this sample, the first whitewash flaking is observed in the 1% drift and near the connection region of beam flange to column flange, Fig. 6. In 2% and 3% drifts, the intensity of flaking is higher near the connection region and towards the middle of flange. In the 3% drift, crack is observed in the connection region of beam flange to the column, in the region of base metal and weld, Fig. 7. By continuing the loading, the cracks become wider; no increase is seen in the cracks length; and whitewash flaking increases severely. In the first cycle of 6% drift, the compressive flange of beam experiences buckling; and in the back loading the test is finished with crack opening.

4.1.3. SP-L sample

In this sample, the first sign of whitewash flaking is observed in the drift of 0.75%, Fig. 6. Concerning 2% drift, flaking is seen in the beam web. By continuing the loading, flaking on the beam flange is more propagated towards the middle of flange and its connection region to the column. The sample experiences crack in the 4% drift at the region connection of beam flange to column, Fig. 7. In the 5% drift, the increasing of whitewash flaking and the opening of crack are significant; and the compressive flange of beam is buckled. The testing of sample is finished in the first cycle of 6% drift by opening the crack.

4.2. Studying the behavior of connection

Fig. 8 presents the hysteresis curves of three samples based on the moment of column face and the whole drift of the story. The moment of column face is calculated through multiplying the measured force applied at the beam end by its distance from column face. The story drift is obtained with respect to FEMA-350 through dividing end beam measured displacement by the distance of beam end from column face plus

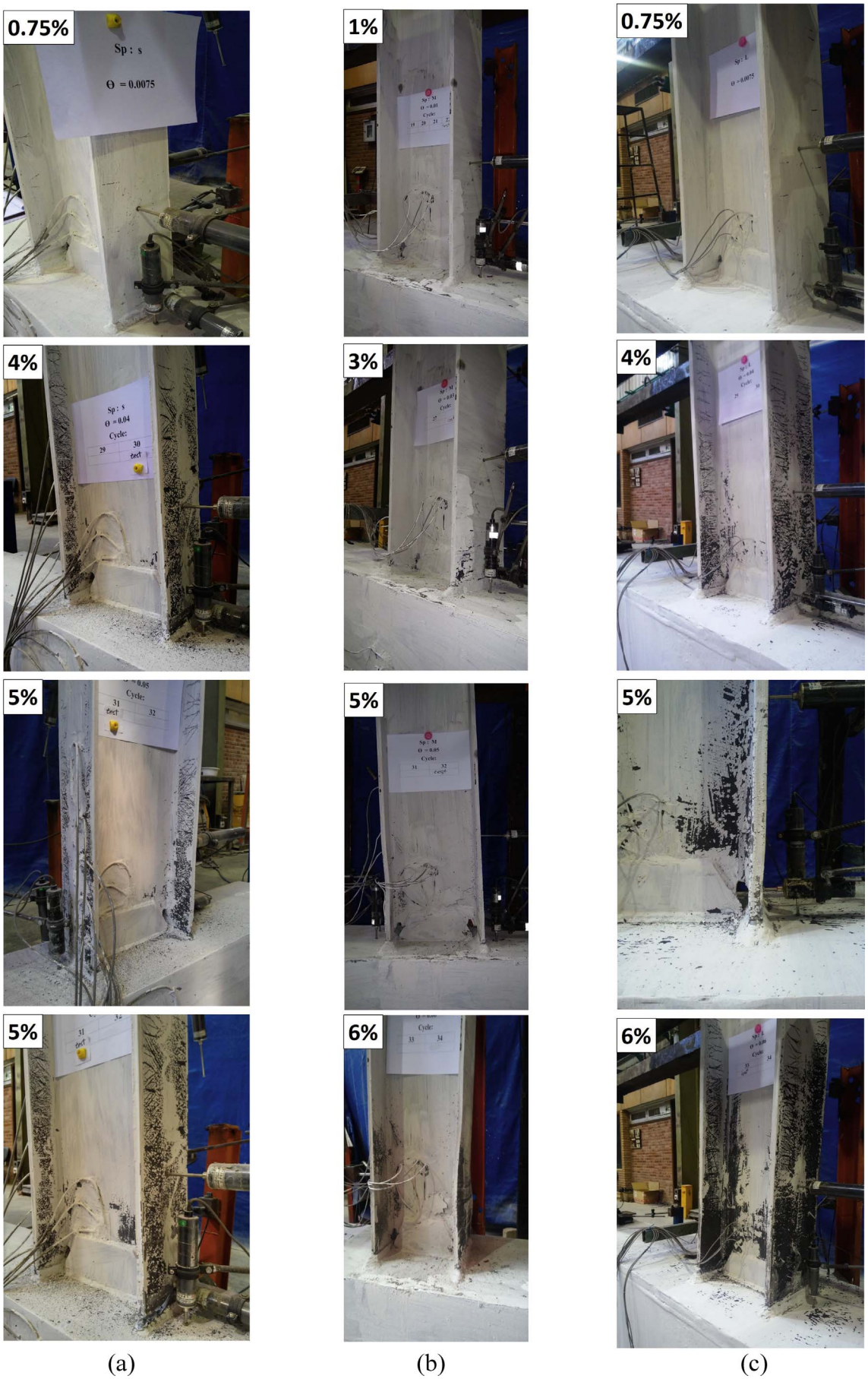

Fig. 6. Observations of test samples: a) SP-S; b) Sp-M; c) SP-L.

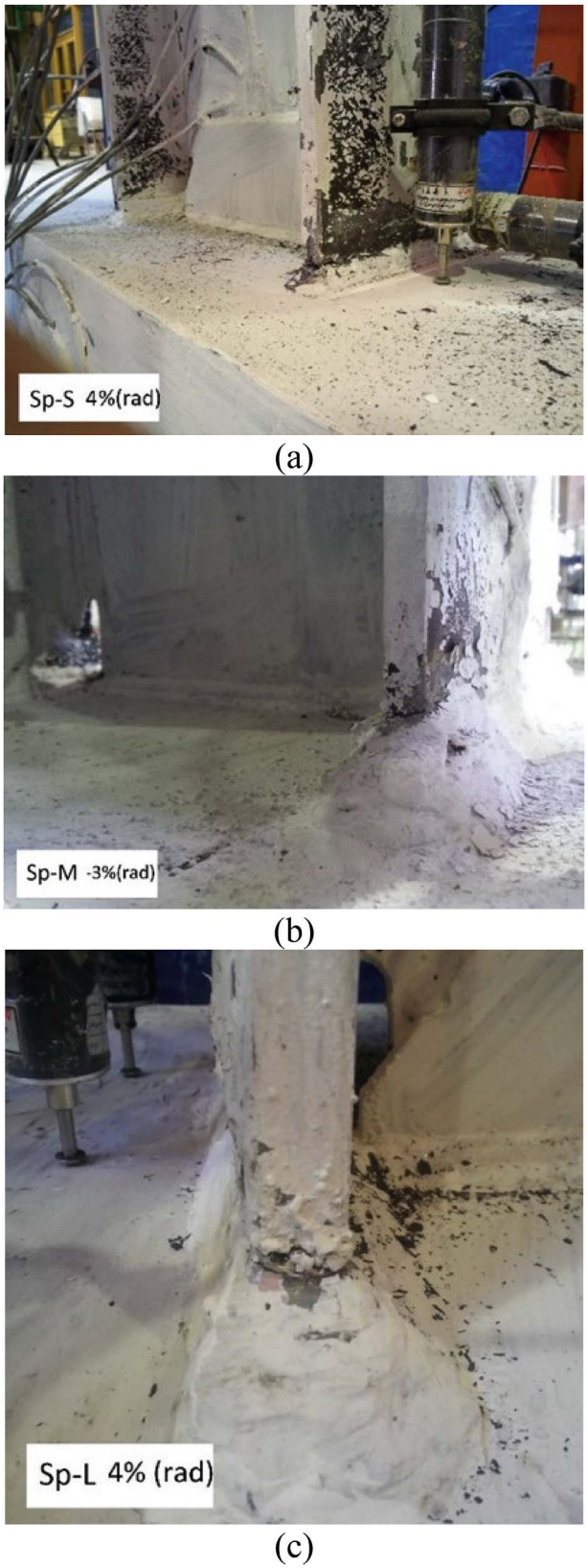

Fig. 7. The cracks initiation observed during the test: a) Sp-S at 4% story drift; b) Sp-M at 3% story drift; c) Sp-L at 4% story drift.

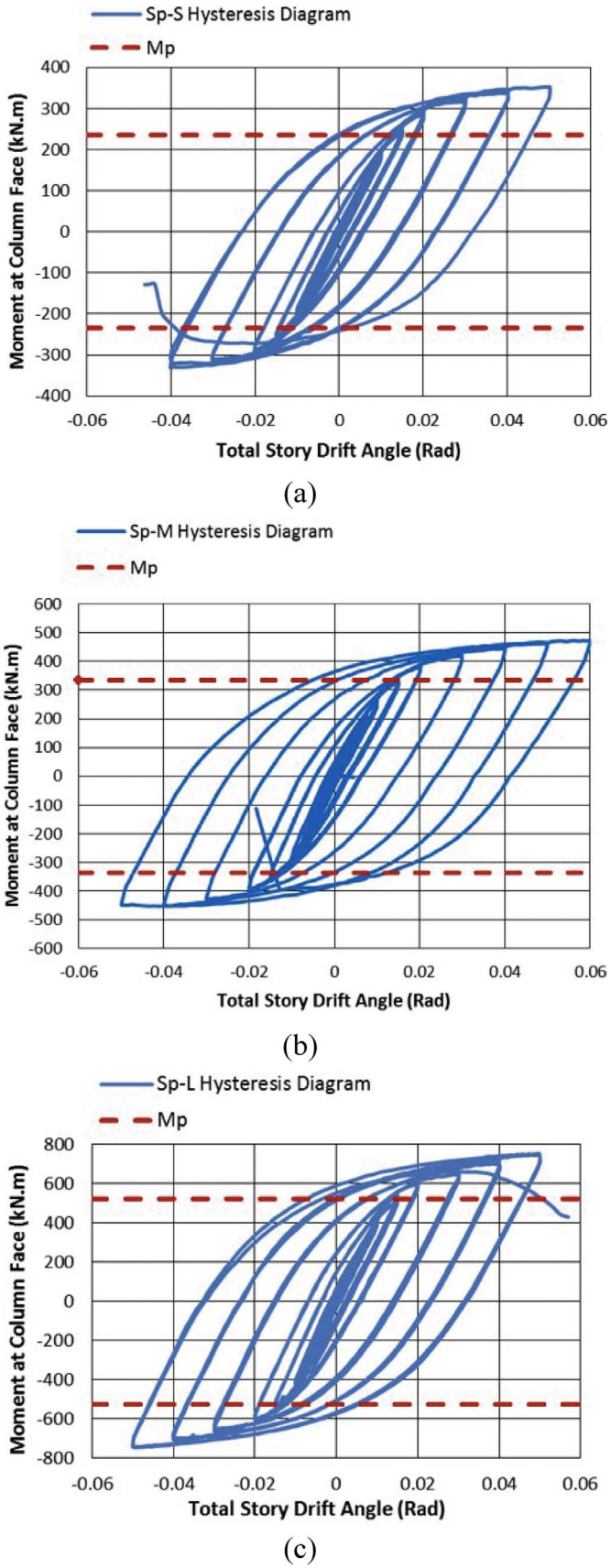

Fig. 8. Hysteresis curve of testing samples: a) Specimen Sp-S; b) Specimen Sp-M; c) Specimen Sp-L.

half of column depth [17]. According to the above mentioned figure, no strength reduction is seen in the samples in 4% drift. Besides, the connection capacity is more than 80% of nominal moment strength of beam. Therefore, the all specimens satisfied special moment resisting

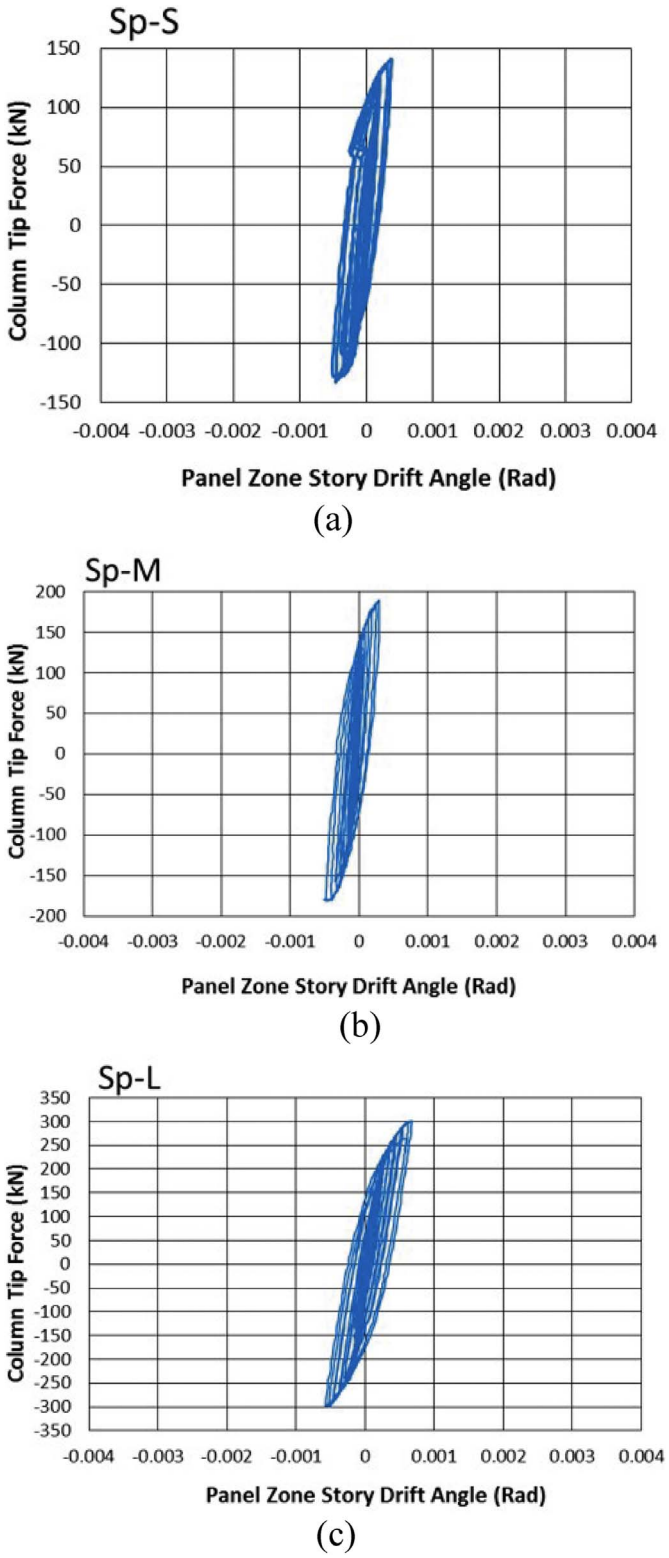

Fig. 9. Panel zone rotation a) Specimen Sp-S; b) Specimen Sp-M; c) Specimen Sp-L.

frames requirements of AISC seismic provision. This code allows maximum strength reduction of 20% in the 4% drift for accepting a connection in the special moment resisting frames. Among the three studied samples, Sp-S and Sp-L show reliable behaviors in the 4% drift. The crack observation in the 3% drift in specimen Sp-M make the behavior unreliable as Fema-350 special moment resisting frames criteria mentioned that no crack observation is allowed before 4% story drift, therefore Sp-M couldn't place in special moment resisting frames.

4.3. Panel zone behavior

No whitewash flaking is observed during the test on the panel zone in all specimens. Two diagonal LVDTs are connected to the panel zone for measuring its deformation during the test. The panel zone deformation in Fig. 9 satisfies the requirements of AISC. Normalized maximum shear strain is calculated using the strains measured by rosette-strain gauges pasted on the panel zones of specimens, shown in Fig. 10.

4.4. Plastic hinge formation

According to the test observation and results, inelastic deformation of beam is the main cause of plastic rotation in all specimens. Strain gauges are pasted on the beam flange in the longitudinal direction for assessing the plastic hinge formation and strains. Fig. 11 presents the longitudinal strains, measured in the length of beam flange. In this figure, the strains are normalized by yield strain. According to this figure, plastic hinge is formed in the samples near the column face, as it is expected for this type of connections, at the distance lower than the width of shear plate. Therefore, it seems that shear plates have no effects on the location of plastic hinge. Plastic hinge is initiated at 3% and 2% story drift in the specimens Sp-S and Sp-L, respectively. Unfortunately, the first row of strain gauges is lost in the specimen Sp-M during the test.

4.5. Initiation and propagation of the crack

Crack initiation in the specimens during the test is reported in laboratory observations, Fig. 7. By continuing the test and applying the load, the cracks become wider with no noticeable increasing in their lengths up to the failure cycle of the connections, especially in the specimen Sp-M that is failed suddenly. The failures of connections are shown in Fig. 12. The strains are measured by the strain gauges pasted on the width of beam flange at the connection region and shown in Fig. 13. The strains at the edge of beam flange have higher values in comparison to those at its middle, considering 4% story drift for specimens Sp-S and Sp-L. This result can explain the locations of crack initiation during the test for these specimens. The curve of strain distribution in the width of beam flange has not been plotted for Sp-M due to losing the strain gauges installed near the beam to column connection region.

5. Discussion

Two possible mechanisms are accepted out of the studied ones and presented in Fig. 1. Considering the acceptability of mechanisms as well as the difference between the thickness values obtained from Eqs. (5) and (10) for a certain connection, the samples are selected for laboratory test in order to properly control the mentioned relations.

Therefore, the thickness of column flange considered for SP-S sample is equal to the needed thickness calculated by Eq. (5), for SP-M sample between the values of Eqs. (5) and (10) and for SP-L higher than those of these two relations.

According to the test results of SP-S and SP-L samples, nonlinear behavior is started in the story drift of 0.75%, and crack is observed in the story drift of 4%. The strength degradation is experienced up to the end of test in the allowable range of AISC-341-10 and FEMA guidelines. Therefore, these two samples are placed in the special flexural frame groups.

Based on the results obtained for SP-M, nonlinear behavior is seen in the story drift of 1% and crack is observed in the story drift of 3%. Moreover, strength degradation remains in the range of AISC-341-10 code up to the end of the test. However, SP-M is not considered as special flexural frame according to FEMA guide line considering the occurrence of crack in the story drift of 4%.

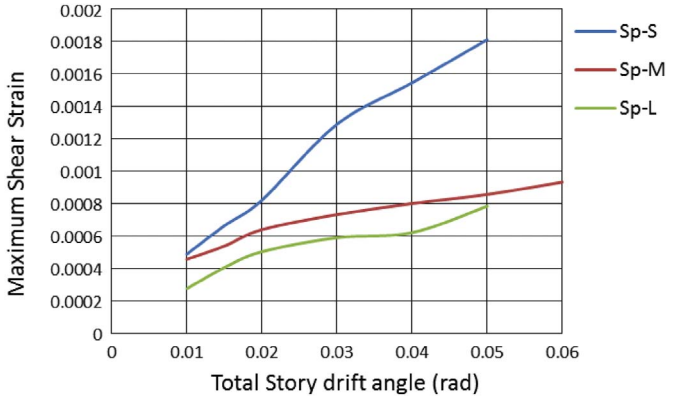

Fig. 10. Maximum shear strain for the specimens.

The samples SP-S and SP-L have the column flange thickness of equal and higher than needed values obtained from Eq. (3). Therefore, it can be concluded that Eq. (5) is appropriate for controlling the necessity of installing the continuity plates in the rigid connection between I-beam and box-column.

According to Fig. 2, back plate with the thickness of 8 mm is used for full penetration groove welding of the connection between bottom flange of beam to column flange. Moreover, 8 mm fillet weld is used as back weld for full penetration groove welding between top flange of beam to column flange. Crack is observed in both connections during the test. However, the connection is finally failed from where the location of mentioned full penetration groove weld with 8 mm fillet back weld.

Based on the laboratory observations, the cracks have no improvement or propagation almost up to the end of test after being formed. The samples experience no strength degradation having the loading capability up to the end of loading. This fact can be due to the redistribution and more uniform of the stress in the width of beam flange considering the reduction of ratio of beam flange width to the box-column flange width after crack formation. In the connection between I-beam and box-column without stiffener, the middle of beam flange may be more deformed comparing to the side regions in the column flange width. Therefore, the edges of beam necessarily experience more concentrated stress and strain. Accordingly, the reduction of ratio of beam flange width to the column flange width can have significant effect on lowering the concentration of stress and strain.

6. Conclusion

This research focuses on the seismic behavior of three moment connections between I-shape beam and box column without continuity plates. The studied connections are of pre-qualified welded unreinforced flange-welded web (WUF-W) moment ones. They were designed according to the relations derived in this research for controlling the necessity of installing the continuity plates and subjected to cyclic loadings. The results obtained from these laboratory investigations are briefly summarized as follows:

The connections have provided the requirements of AISC seismic provisions and therefore can be categorized in the rigid connections. Regarding the elasticity of panel zone, energy dissipation of column flange and crack observing during the test in the corner regions of beam flange at the column face, connection failure mode can be changed from ductile to brittle.

While no continuity plates were installed in these connections, they provide the conditions of special moment resisting frames. Therefore, the installation of continuity plates in the box column can be ignored in case of providing some special conditions in the panel zone.

The thickness values are selected for three tested samples, Sp-S, Sp-M and Sp-L, as equal, lower and higher than the thickness calculated by Eq. (5), respectively. According to the results obtained from laboratory

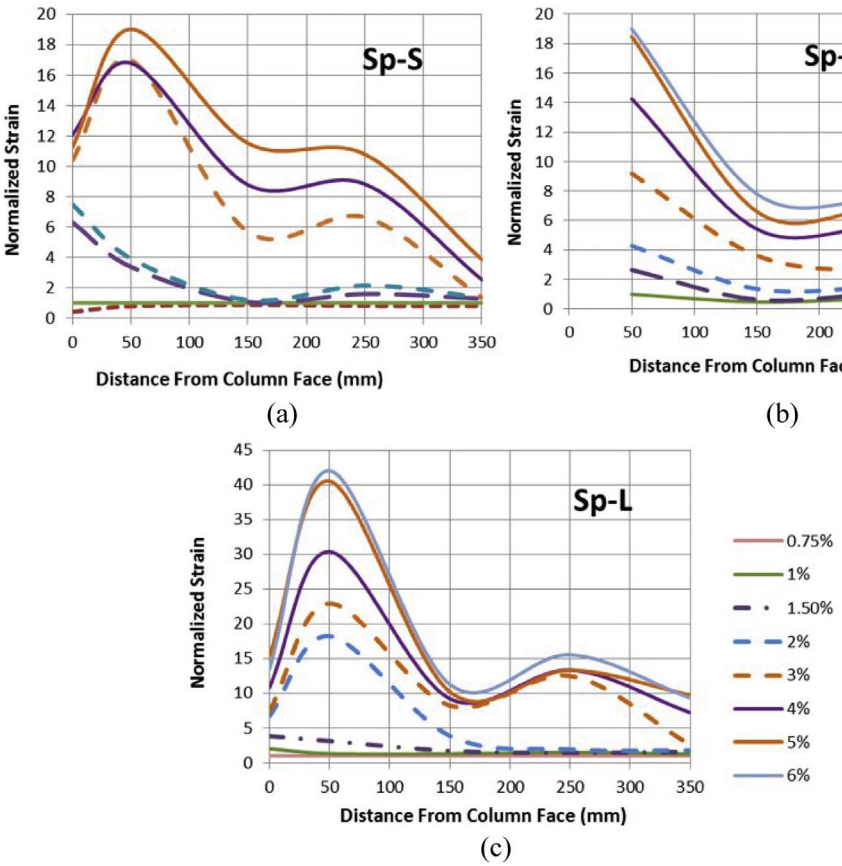

Fig. 11. Maximum normalized strain in the length of upper flange: a) Specimen Sp-S; b) Specimen Sp-M; c) Specimen Sp-L.

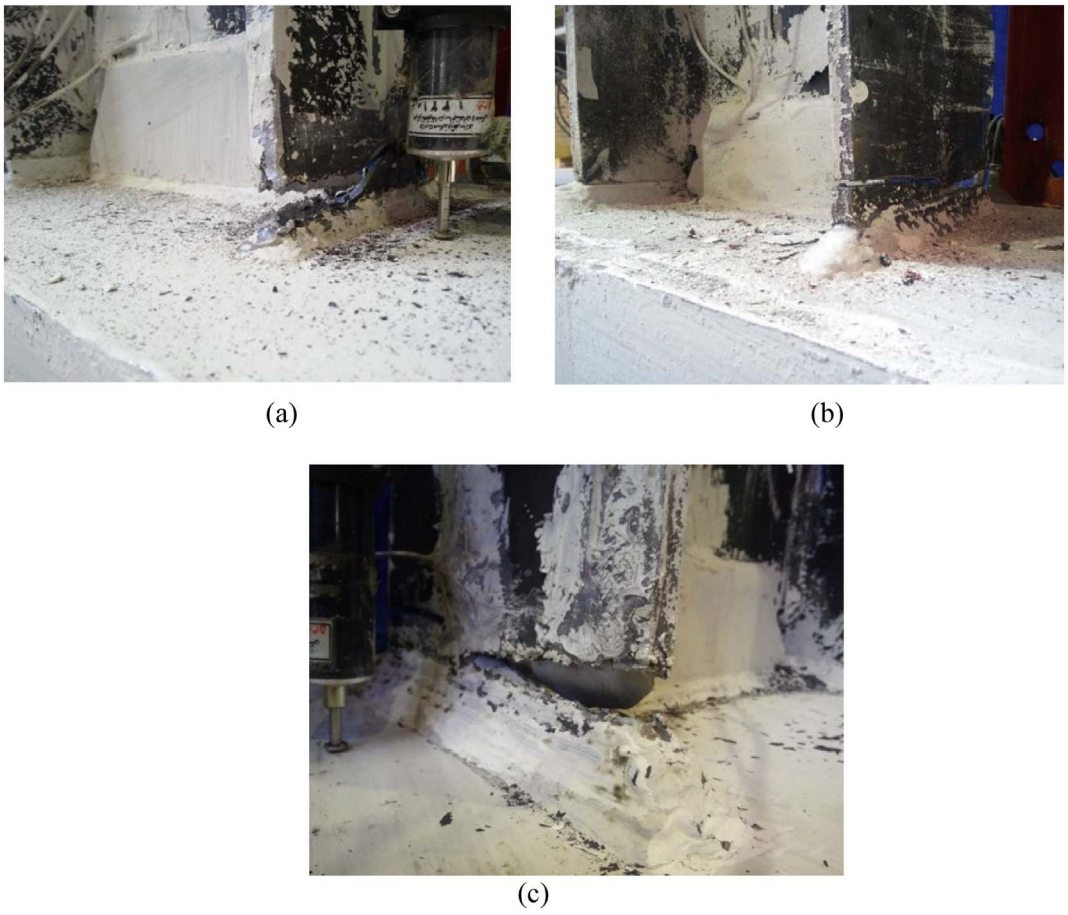

Fig. 12. Connections failure a) specimen Sp-S at 5% drift b) specimen Sp-M at 6% drift c) specimen Sp-L at 6% drift.

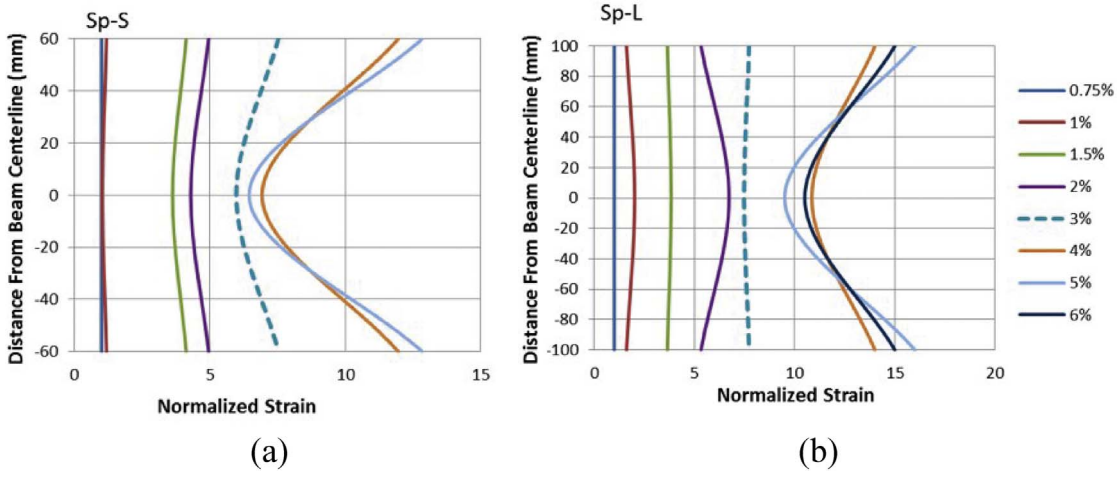

Fig. 13. Maximum normalized strain in the width of beam flange a) Specimen Sp-S b) Specimen Sp-L.

tests, Eq. (5) is suggested for controlling the necessity of installing the continuity plates in the rigid connections between I-shape beams and box columns;

Eq. (5) is obtained using local bending control of box column flange connected to I-shape beam. It has been verified through laboratory tests and therefore is suggested for controlling the local bending of box column flange.

References

[1] Sara D. Prochnow, Robert J. Dexter, Jerome F. Hajjar, Yanqun Ye, Sean C. Cotton, Local flange bending and local web yielding limit states in steel moment-resisting connections, Structural Engineering Report No. ST-00-4, 2000.
[2] AISC, Seismic Provisions for Structural Steel Buildings, AISC, 1997.
[3] AISC, Load and Resistance Factor Design Specification for Structural Steel Buildings, AISC, 1999.
[4] R. Tremblay, P. Timler, M. Bruneau, A. Filiatrault, Performance of steel structures during the 1994 Northridge earthquake, Can. J. Civ. Eng. 22 (1995) 338–360.
[5] E.J. Kaufmann, M. Xue, L.W. Lu, J.W. Fisher, Achieving ductile behavior of moment connections, Mod. Steel Constr. 36 (1) (1996) 30–39. AISC.
[6] C.W. Roeder, An evaluation of cracking observed in steel moment frames, in: L. Kempner, C. Brown (Eds.), Proceedings of the ASCE Structures Congress, 1997 Portland, Oregon.
[7] R.K. Yee, S.R. Paterson, G.R. Egan, Engineering evaluations of column continuity plate detail design and welding issues in welded steel moment frame connections, Welding for Seismic Zones in New Zealand, Aptech Engineering Services, Inc., Sunnyvale, California, 1998.

[8] M.D. Engelhardt, B.D. Shuey, T.A. Sabol, Testing of repaired steel moment connections, in: L. Kempner, C. Brown (Eds.), Proceedings of the ASCE Structures Congress, 1997 Portland, Oregon.
[9] J.M. Ricles, L. Mao, E.J. Kaufmann, L. Lu, J.W. Fisher, Development and Evaluation of Improved Details for Ductile Welded Unreinforced Flange Connections, SAC BD 00-24, SAC Joint Venture, 2000.
[10] M.S. Ghobadi, M. Ghassemieh, A. Mazroi, A. Abolmaali, Seismic Performance of Ductile Welded Connections Using T-stiffener, J. Constr. Steel Res., 2009.
[11] Roozbeh Kiamanesh, Ali Abolmaali, Mehdi Ghassemieh, The Effect of Stiffeners on the Strain Patterns of the Welded Connection Zone, Journal of Constructional Steel Research, 2010.
[12] Seyed Rasoul Mirghaderi, Shahabeddin Torabian, Farhad Keshavarzi, I-beam to Box–column Connection by a Vertical Plate Passing Through the Column, Engineering Structures, 2010.
[13] Shahabeddin Torabian, Seyed Rasoul Mirghaderi, Farhad Keshavarzi, Moment-connection between I-beam and built-up square column by a diagonal through plate, J. Constr. Steel Res. 70 (March 2012) 385–401.
[14] J.D. Graham, A.N. Sherbourne, R.N. Khabbaz, C.D. Jensen, Welded Interior Beam-to-column Connections, Welding Research Council, 1960.
[15] AISC, Seismic Provisions for Structural Steel Buildings, AISC, 2010.
[16] Z. Saneei Nia, M. Ghassemieh, A. Mazroi, WUF-W connection performance to box column subjected to uniaxial and biaxial loading, J. Constr. Steel Res. 88 (September 2013) 90–108.
[17] FEMA, Recommended Seismic Design Criteria for New Steel Moment-frame Buildings, FEMA 350, Federal Emergency Management Agency, 2000.